



HAL
open science

Validation of THz absorption spectroscopy by a comparison with ps-TALIF measurements of atomic oxygen densities

J R Wubs, L. Invernizzi, K. Gazeli, U. Macherius, X. Lü, L. Schrottke, G. Lombardi, K.-D. Weltmann, J H van Helden

► To cite this version:

J R Wubs, L. Invernizzi, K. Gazeli, U. Macherius, X. Lü, et al.. Validation of THz absorption spectroscopy by a comparison with ps-TALIF measurements of atomic oxygen densities. *Applied Physics Letters*, 2023, 123 (8), pp.081107. 10.1063/5.0160303 . hal-04228688

HAL Id: hal-04228688

<https://hal.science/hal-04228688v1>

Submitted on 4 Oct 2023

HAL is a multi-disciplinary open access archive for the deposit and dissemination of scientific research documents, whether they are published or not. The documents may come from teaching and research institutions in France or abroad, or from public or private research centers.

L'archive ouverte pluridisciplinaire **HAL**, est destinée au dépôt et à la diffusion de documents scientifiques de niveau recherche, publiés ou non, émanant des établissements d'enseignement et de recherche français ou étrangers, des laboratoires publics ou privés.



Distributed under a Creative Commons Attribution 4.0 International License

RESEARCH ARTICLE | AUGUST 22 2023

Validation of THz absorption spectroscopy by a comparison with ps-TALIF measurements of atomic oxygen densities ^{EP}

J. R. Wubs ; L. Invernizzi ; K. Gazeli ; U. Macherius ; X. Lü ; L. Schrottke ; G. Lombardi ; K.-D. Weltmann ; J. H. van Helden 

 Check for updates

Appl. Phys. Lett. 123, 081107 (2023)

<https://doi.org/10.1063/5.0160303>



View Online



Export Citation

CrossMark

Articles You May Be Interested In

Picosecond two-photon absorption laser-induced fluorescence (ps-TALIF) in krypton: The role of photoionization on the density depletion of the fluorescing state $Kr\ 5p[3/2]_2$

Phys. Plasmas (April 2021)

O₃ full photo-fragmentation TALIF spectroscopy for quantitative diagnostics of non-thermal O₂-mixed plasmas

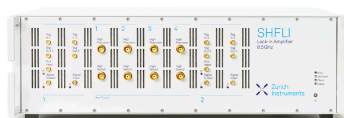
J. Appl. Phys. (April 2023)

Novel xenon calibration scheme for two-photon absorption laser induced fluorescence of hydrogen

Rev. Sci. Instrum. (July 2016)

500 kHz or 8.5 GHz?
And all the ranges in between.

Lock-in Amplifiers for your periodic signal measurements



Find out more



Validation of THz absorption spectroscopy by a comparison with ps-TALIF measurements of atomic oxygen densities

Cite as: Appl. Phys. Lett. **123**, 081107 (2023); doi: [10.1063/5.0160303](https://doi.org/10.1063/5.0160303)

Submitted: 31 May 2023 · Accepted: 4 August 2023 ·

Published Online: 22 August 2023 · Publisher error corrected: 23 August 2023



View Online



Export Citation



CrossMark

J. R. Wubs,^{1,a)}  L. Invernizzi,²  K. Gazeli,²  U. Macherius,¹  X. Lü,³  L. Schrottke,³  G. Lombardi,² 
K.-D. Weltmann,¹  and J. H. van Helden¹ 

AFFILIATIONS

¹Leibniz Institute for Plasma Science and Technology (INP), Felix-Hausdorff-Straße 2, 17489 Greifswald, Germany

²Laboratoire des Sciences des Procédés et des Matériaux (LSPM), CNRS, Université Sorbonne Paris Nord, UPR 3407, F-93430 Villetaneuse, France

³Paul-Drude-Institut für Festkörperelektronik, Leibniz-Institut im Forschungsverbund Berlin e. V., Hausvogteiplatz 5-7, 10117 Berlin, Germany

^{a)} Author to whom correspondence should be addressed: jente.wubs@inp-greifswald.de

ABSTRACT

Terahertz (THz) absorption spectroscopy has recently been developed as a diagnostic technique for measuring absolute ground-state atomic oxygen densities in plasmas. To demonstrate the validity of this approach, we present in this Letter a benchmark against a more established method. Atomic oxygen densities were measured with THz absorption spectroscopy and compared to those obtained from picosecond (ps) two-photon absorption laser induced fluorescence (TALIF) measurements on the same capacitively coupled radio frequency oxygen discharge. Similar changes in the atomic oxygen density were observed with both diagnostics when varying the applied power (20–100 W) and the gas pressure (0.7–1.3 mbar). Quantitatively, the results are in good agreement as well, especially when considering the total margin of error of the two diagnostics. For example, for a gas pressure of 1.3 mbar and an applied power of 30 W, atomic oxygen densities measured with THz absorption spectroscopy and TALIF were $(7.0 \pm 1.7) \times 10^{14} \text{ cm}^{-3}$ and $(5.3 \pm 3.2) \times 10^{14} \text{ cm}^{-3}$, respectively. This shows that THz absorption spectroscopy is an accurate technique that can be reliably used for real-world applications to determine atomic oxygen densities in plasmas.

© 2023 Author(s). All article content, except where otherwise noted, is licensed under a Creative Commons Attribution (CC BY) license (<http://creativecommons.org/licenses/by/4.0/>). <https://doi.org/10.1063/5.0160303>

Plasmas containing oxygen are used in a variety of applications, including biological decontamination,¹ modification of polymer surfaces,^{2–4} removal of photoresist,⁵ catalysis,^{6,7} and plasma-assisted nanofabrication.^{8,9} As oxygen atoms are a key species in most of these plasmas, knowledge on their densities is crucial to better understand the plasma chemistry and improve industrial processes. Frequently used methods to determine atomic oxygen densities include two-photon absorption laser induced fluorescence (TALIF)^{10–12} and actinometry.^{13,14} However, TALIF is rather expensive and requires a complex calibration procedure involving a comparison between two-photon absorption cross sections of oxygen and xenon,^{15,16} whereas actinometry relies upon many assumptions and possibly perturbs the plasma.

An alternative method is provided by terahertz (THz) absorption spectroscopy. The possibility to employ this diagnostic technique has

been opened up by the increasing availability of suitable THz sources and detectors.^{17–21} Recently, we have demonstrated the first implementation of THz absorption spectroscopy to measure atomic oxygen densities in plasmas.²² The measurement principle is based on the detection of the $^3P_1 \leftarrow ^3P_2$ fine structure transition of ground-state atomic oxygen at approximately 4.75 THz, using a tunable quantum cascade laser (QCL) as THz source^{17,18} and a bolometer for detection. One of the main advantages of THz absorption spectroscopy is that it allows for direct measurements (i.e., no calibration procedure required) of absolute ground-state atomic oxygen densities. Its accuracy depends almost exclusively on the accuracy to which the transition line strength is known. In addition, the experimental setup for THz absorption spectroscopy is relatively compact,¹⁸ especially compared to TALIF setups that typically involve bulky laser systems.

The requirements for the optical alignment are not as strict as for cavity ringdown spectroscopy (CRDS),²³ and vacuum conditions are not essential, making THz absorption spectroscopy experimentally less challenging than vacuum ultraviolet (VUV) absorption spectroscopy.²⁴ Furthermore, the high spectral resolution and narrow laser linewidth (below 10 MHz) make it possible to reliably determine the temperature of oxygen atoms from the measured absorption profiles as well. These features make THz absorption spectroscopy an attractive diagnostic for atomic oxygen density measurements in plasmas. However, it cannot compete with the high spatial and temporal resolutions of TALIF measurements, mainly because yielded results are typically line-of-sight integrated. THz absorption spectroscopy is, therefore, most suited for measurements on non-transient plasmas with a well-defined density distribution.

In this Letter, THz absorption spectroscopy is benchmarked against TALIF measurements, as this is currently the most established method for measuring atomic oxygen densities.¹⁰ To this end, both THz absorption spectroscopy and picosecond (ps) TALIF measurements were performed on the same capacitively coupled radio frequency (CCRF) discharge generated in pure oxygen for a variation of the applied RF power (20–100 W) and the gas pressure (0.7–1.3 mbar).

The experimental setup for THz absorption spectroscopy is schematically depicted in Fig. 1(a). The investigated absorption transition is the ${}^3P_1 \leftarrow {}^3P_2$ transition between two of the fine structure levels of ground-state atomic oxygen, as shown in Fig. 1(b) (top). The transition frequency is 4.744 777 49 THz (corresponding to $158.268\,741\text{ cm}^{-1}$).²⁵ A tunable, continuous-wave THz QCL with an output power of approximately 4 mW was used as THz source.^{17,18} It was operated in a Stirling cryocooler (Ricor K535) at a temperature of 43.3 K. Temperature fluctuations were minimized to be below 5 mK by an additional temperature controller (Stanford Research Systems, CTC100). Tuning of the laser output was achieved by linearly ramping the input current (tuning coefficient: $7.8 \times 10^{-4}\text{ cm}^{-1}/\text{mA}$).

The current was supplied by a laser driver (Wavelength Electronics, QCL1000 OEM), which was controlled by a function generator (Tektronix, AFG3022C) to provide sawtooth waveforms with a slope of 74.8 mA/s and a frequency of 11 Hz. The laser beam with a diameter of $(3 \pm 1)\text{ mm}$ (full width at half maximum) was guided through the plasma reactor as indicated in Fig. 1(a). The part of the laser beam path outside the plasma reactor was purged with nitrogen gas to minimize the absorption by atmospheric water vapor. An etalon or reference gas cell (RGC) could be placed in the beam path to characterize the laser tuning properties and laser linewidth; this is described in more detail elsewhere.²² The THz radiation was detected by a helium-cooled bolometer (Infrared Laboratories, 4.2K Bolometer). A phase-locked optical chopper (New Focus, Model 3502) with a frequency of 5.5 Hz was used to block each second period of the laser output. The detected signals were recorded with a digital sampling oscilloscope (R&S, RTO 1014), and all results presented in this Letter were averaged over 100 individual measurements to improve the signal-to-noise ratio (total measurement time of approximately 10 s).

The plasma used for the investigations is an asymmetric CCRF oxygen discharge similar to the one used in previous work.²² The planar RF electrode had a diameter of 120 mm and was positioned at a distance of 55 mm beneath the top surface of the grounded reactor vessel, which had a diameter of 240 mm and a height of 105 mm. Power (20–100 W at 13.56 MHz) was delivered by an RF generator (Advanced Energy, Cesar 133) and an automatic matching network (Advanced Energy, Navio). The reactor outlet was connected to a turbopump system (Welch-Ilmvac, CDK 263) with a throttle valve to constantly adjust the pressure in the chamber to 0.7 or 1.3 mbar. Oxygen gas was let into the reactor by a mass flow controller (MFC) (MKS 1179A with control unit MKS PR4000) at a flow rate of 45 or 50 sccm, respectively.

The experimental setup for performing ps-TALIF measurements on the same plasma reactor is shown in Fig. 1(c). The two-photon excitation scheme of the investigated fluorescence transition is given in Fig. 1(b) (bottom). Photons with a wavelength of approximately

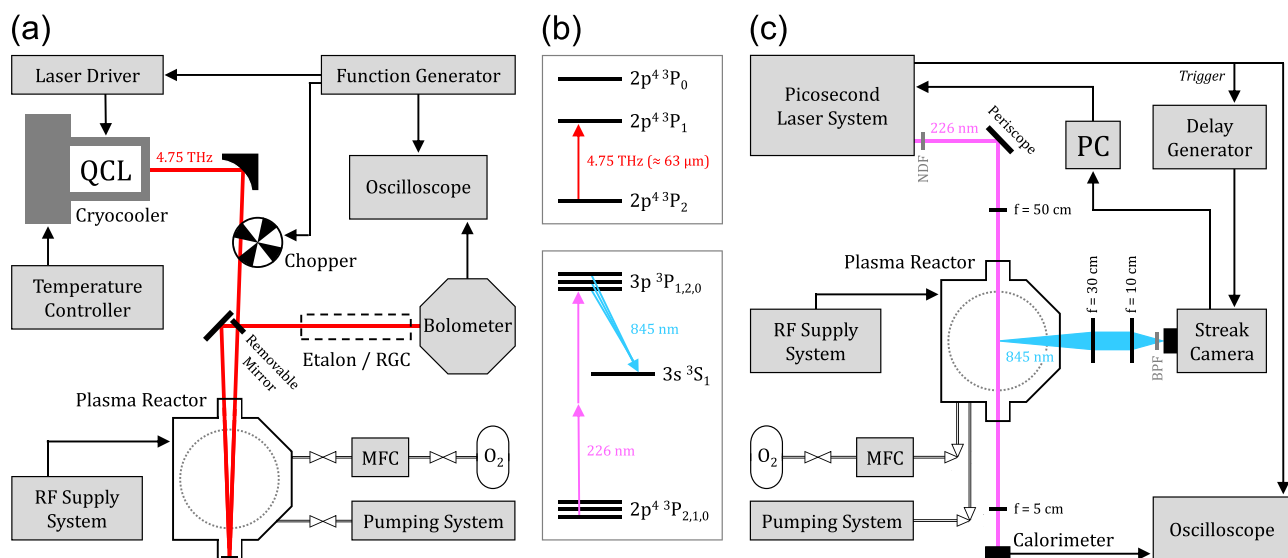


FIG. 1. Schematic representation of the experimental setups used for (a) THz absorption spectroscopy and (c) ps-TALIF measurements, with (b) the corresponding excitation schemes of the investigated atomic oxygen transitions.

226 nm were provided by a ps laser system that consisted of an Nd:YLF pump laser (EKSPLA, PL3140), a harmonic generator (EKSPLA, APL2100), and an optical parametric generator (EKSPLA, PG411). More details on this laser system can be found elsewhere.²⁶ Neutral density filters (NDFs) were placed in front of the laser output to attenuate the laser beam. The laser energy was monitored by a calorimeter (Coherent, J-10MB-LE) connected to an oscilloscope (Teledyne Lecroy, Wavesurfer 10). The fluorescent radiation, with a wavelength of approximately 845 nm, was detected perpendicular to the direction of the laser beam by a streak camera (HAMAMATSU, C10910-05) to record the spatiotemporal development of the TALIF signal. Technical details on this method of detection can be found in the work of Invernizzi *et al.*²⁷ The streak camera was synchronized with the laser pulses (repetition rate: 5 Hz) by a delay generator (Stanford Research, DG645) and connected to a digital CMOS camera for readout (HAMAMATSU, ORCA-Flash4.0 V3). The fluorescent radiation was focused on the horizontally oriented entrance slit (width: 100 μm) with a magnification of 0.25. A bandpass filter (BPF), with a bandwidth of 21 nm centered around 840 nm, was used to filter for only the fluorescence wavelength. The streak camera images were recorded using a time range of 200 ns, full gain, and a total acquisition time of 200 s, which corresponds to an accumulation of 1000 laser shots. Temporal information was extracted from the images spatially averaged over the full image range, i.e., over a length of approximately 15 mm.

Figure 2(a) shows a typical example of a time-resolved TALIF signal, measured for a laser wavelength of 225.555 nm, a gas pressure of 1.3 mbar, and an applied RF power of 30 W. The exponential decay directly provides the effective lifetime τ_{eff} of oxygen atoms in the excited state $3p^3P_J$. Effective lifetimes were determined to be approximately 21 and 17 ns at 0.7 and 1.3 mbar, respectively, with minor changes when varying the applied RF power. Integration over time for different laser wavelengths resulted in a spectral profile such as shown in Fig. 2(b). It was fitted by a Gaussian function, although a slight asymmetry can be observed; this was due to contributions from the $3p^3P_{1,2,0}$ fine structure levels, as the laser linewidth (approximately 28 pm) was insufficiently narrow to distinguish between them. The spectrally integrated TALIF signal S_F (i.e., the area under the Gaussian fit) is proportional to the ground-state atomic oxygen density; however, a calibration using xenon gas is required to obtain absolute ground-state densities. This calibration method is widely used and well-explained in the literature.^{10,11,15,16,28–30} The density of oxygen atoms in the $2p^4^3P_2$ state was obtained by comparing fluorescence intensities measured for oxygen and xenon

$$n_{\text{O}(2p^4^3P_2)} = C \frac{S_{\text{F}}^{\text{O}} \tau_{\text{eff}}^{\text{Xe}} \left(\frac{E_{\text{laser}}^{\text{Xe}}}{E_{\text{laser}}^{\text{O}}} \right)^2}{S_{\text{F}}^{\text{Xe}} \tau_{\text{eff}}^{\text{O}}} \quad (1)$$

Here, E_{laser} is the laser energy, and C a calibration constant involving various invariant parameters, such as the two-photon absorption cross sections and natural lifetimes of oxygen and xenon.¹⁰ In this work, the following value for the two-photon absorption cross section ratio was used:

$$\frac{\sigma_{\text{Xe}}}{\sigma_{\text{O}}} = 1.02 (\pm 50\%), \quad (2)$$

which is based on the cross sections of oxygen and xenon reported by Bamford *et al.*³¹ and Drag *et al.*,³² respectively. The natural lifetime of

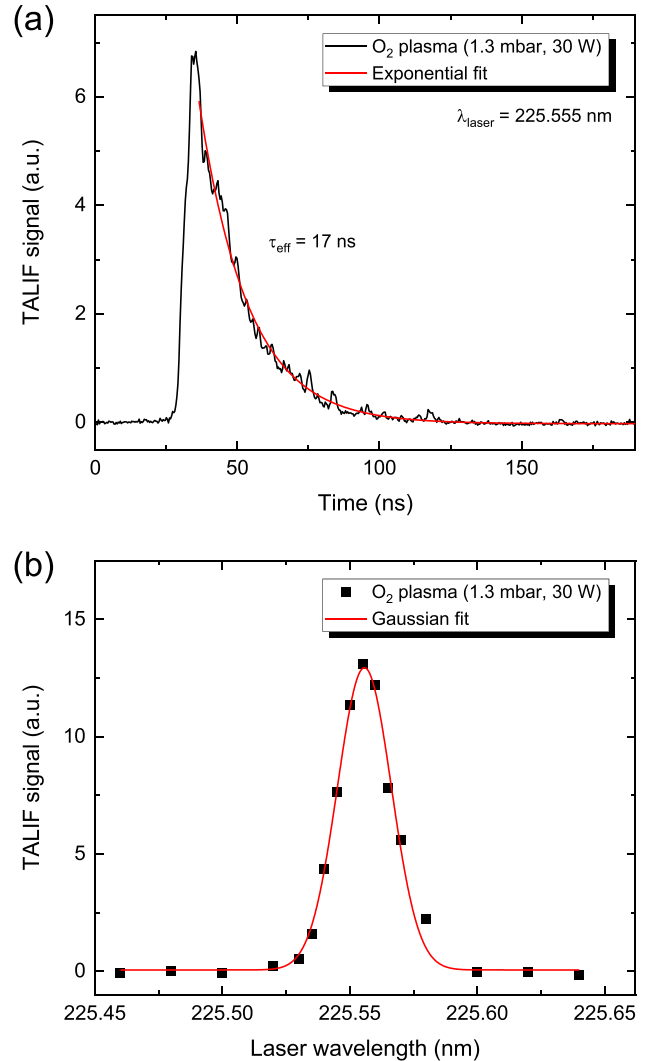


FIG. 2. (a) Time-resolved $3p^3P_J \rightarrow 3s^3S_1$ TALIF signal for a laser wavelength of 225.555 nm and (b) spectral profile of the time-integrated TALIF signal, measured in a CCRF O₂ discharge for a gas pressure of 1.3 mbar and an applied RF power of 30 W.

the excited state $\text{Xe}(6p'[3/2]_2)$ was measured to be 32.8 ns ($\pm 25\%$)¹⁰, while the natural lifetime of the excited state $\text{O}(3p^3P_J)$ was taken from the work of Bamford *et al.*,³¹ who reported a value of 34.7 ns ($\pm 11\%$). Furthermore, a sufficiently low laser energy had to be selected to ensure that no saturation effects (e.g., photo-ionization, photo-dissociation, and stimulated emission) occur.¹⁰ Therefore, several measurements were done to determine the non-saturation regime, which is characterized by a quadratic dependence of the TALIF signal on the laser energy, and laser energies were chosen well below the saturation limit. For the calibration with xenon, results were averaged over five measurements with different laser energies in the range from 0.4 to 1.0 μJ . The atomic oxygen measurements were done with a laser energy of 3–4 μJ , and the densities presented further on in this Letter all represent the average of five single measurements using the peak excitation

method described by Bisceglia *et al.*,³³ as it could be shown that the results obtained with this method are in excellent agreement with those obtained from the full spectral profile (comparison not shown here). Total ground-state densities were calculated from the measured $O(2p^4\ ^3P_2)$ densities by assuming that the fine structure levels are in thermal equilibrium and populated according to a Boltzmann distribution.

Figure 3 shows a typical example of a spectral absorption profile of atomic oxygen, obtained with THz absorption spectroscopy under the same plasma conditions as the TALIF signal shown in Fig. 2. The shape of the spectral profile was determined by Doppler and instrumental broadening, and it could be described with a Gaussian function. The width of the instrumental broadening contribution was $2 \times 10^{-4} \text{ cm}^{-1}$ ($\pm 25\%$).²² As this is narrower than the Doppler width (typically 5 to $6 \times 10^{-4} \text{ cm}^{-1}$), the temperature of the oxygen atoms could be reliably determined from the Gaussian width of the fit.³⁴ This could be done with a much better accuracy compared to previous work²² due to several improvements of the experimental setup. These included purging a part of the setup with nitrogen gas and choosing a different laser tuning frequency (11 instead of 10 Hz), which led to a significantly better signal-to-noise ratio and a reduction of signal disturbances, and hence an improved quality of the Gaussian fit. The obtained temperatures were approximately 365 and 440 K ($\pm 12\%$) at 0.7 and 1.3 mbar, respectively, with no evident influence of the applied RF power. Although the TALIF spectral profiles were affected by the same broadening mechanisms, it was impossible to deduce the temperature from spectral profiles such as the one shown in Fig. 2(b); the reason for this is that the laser linewidth of the ps laser (approximately 28 pm, i.e., 5.5 cm^{-1}) was significantly broader than that of the THz QCL and dominating over the Doppler broadening.

According to the Lambert–Beer law, the integrated absorbance (i.e., the area under the Gaussian fit in Fig. 3) is directly proportional to the absolute density n_O of ground-state atomic oxygen,

$$\int_{\text{line}} \text{Absorbance } d\nu = n_O L S(T), \quad (3)$$

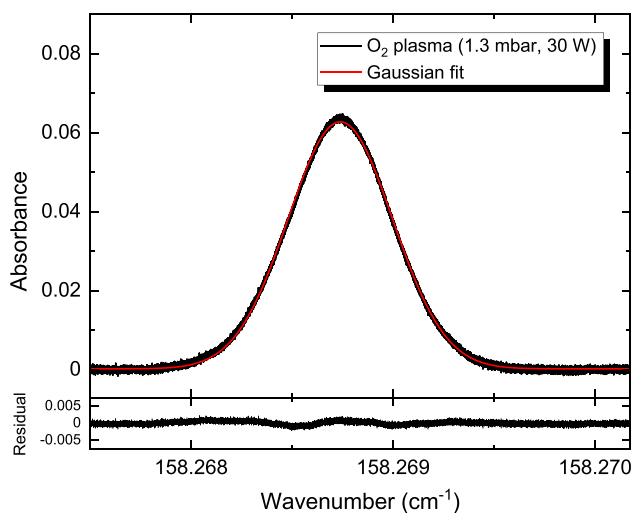


FIG. 3. Gaussian-shaped spectral absorption profile of the $^3P_1 \leftarrow ^3P_2$ fine structure transition of ground-state atomic oxygen, measured in a CCRF O_2 discharge for a gas pressure of 1.3 mbar and an applied RF power of 30 W.

where L is the absorption length, and S the line strength.³⁴ The line strength of the investigated atomic oxygen transition was reported to be $1.117 \times 10^{-21} \text{ cm}^{-1}/(\text{molecule cm}^{-2})$ at a reference temperature of 296 K (no uncertainty in S given).^{35,36} Temperature-specific values were calculated to be 0.92×10^{-21} and $0.78 \times 10^{-21} \text{ cm}^{-1}/(\text{molecule cm}^{-2})$ at 365 and 440 K, respectively.³⁷ The temperature dependence of the line strength involves the same Boltzmann factor as used for the ps-TALIF measurements to convert $O(2p^4\ ^3P_2)$ densities into total ground-state atomic oxygen densities. In addition, it takes into account the non-negligible effect of stimulated emission from the 3P_1 to the 3P_2 state.³⁷ For this reason, small changes in the temperature generally have a significantly larger impact on total atomic oxygen densities obtained with THz absorption spectroscopy than on those obtained with TALIF.

As absorption spectroscopy is a line-of-sight integrated technique, atomic oxygen densities determined with THz absorption spectroscopy typically represent the average density along the absorption length L . It could, however, be assumed that the oxygen atoms were distributed homogeneously throughout the reactor volume, such that the line-of-sight integrated densities measured with THz absorption spectroscopy should differ only marginally from the spatially resolved ones measured with TALIF. This assumption was supported by TALIF measurements done at different heights above the powered electrode (in the range from 2 to 30 mm), showing no distinct impact of the electrode proximity on the density of atomic oxygen (results not shown). Therefore, a value of $(84 \pm 2) \text{ cm}$ was taken for the absorption length [i.e., twice the window-to-mirror distance, see Fig. 1(a)]. It could, however, not be confirmed if the density distribution along the laser line of sight was indeed homogeneous, as the small size of the window for observation of the fluorescent radiation did not allow for density measurements more than 3 cm away from the center of the plasma reactor.

The deviation between the spectral absorption profile presented in previous work²² and the one shown in Fig. 3 was caused by a slight difference in plasma conditions (a flow rate of 70 instead of 45–50 sccm), possibly in combination with a part of the THz radiation passing through the reactor multiple times, which would result in an unanticipated increase in the absorption length, and hence an overestimation of the atomic oxygen density. In this work, the reactor windows were attached under an angle to avoid this unwanted effect.

Figure 4 shows a comparison between absolute ground-state atomic oxygen densities obtained from THz absorption spectroscopy and ps-TALIF measurements for gas pressures of 0.7 and 1.3 mbar and a variation of the applied RF power from 20 to 100 W. All data points represent the average of five individual measurements. The vertical bars indicate the standard deviation (i.e., not the total error) and, hence, demonstrate the reproducibility of the observed trends. Relatively large spreads in the results were observed mainly for applied RF powers above approximately 70 W. For a gas pressure of 1.3 mbar, this was attributed to an unstable discharge behavior. For a gas pressure of 0.7 mbar, the larger spreads in the TALIF results for higher applied RF powers were a consequence of the low signal intensity in combination with the more intense background radiation emitted by the plasma.

In general, increasing the gas pressure led, as expected, to higher atomic oxygen densities, while a slight decrease in the atomic oxygen density was observed with increasing applied RF power. Similar trends

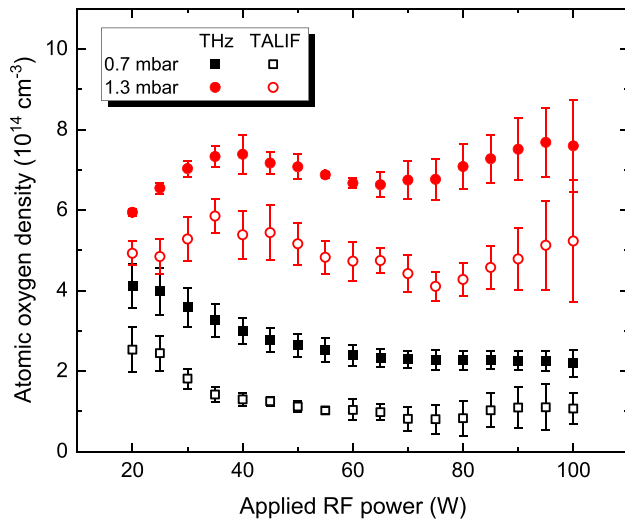


FIG. 4. Comparison between absolute atomic oxygen densities obtained from THz absorption spectroscopy and ps-TALIF measurements on the same CCRF O₂ discharge for a variation of the applied RF power and the gas pressure. All data points represent the average of five single measurements; the vertical bars indicate the standard deviation. Systematic errors are approximately 25% for THz absorption spectroscopy and 60% for TALIF.

in atomic oxygen densities were obtained with both diagnostics. The plasma chemical processes underlying these trends are not the focus of this Letter but will be investigated in the future by means of a comparison with modeling.

Quantitatively, the results obtained with THz absorption spectroscopy and TALIF are in good agreement as well, especially when considering the total margin of error of the two diagnostics. Total systematic errors were calculated to be 25% and 60% for THz absorption spectroscopy and TALIF, respectively, based on a quadratic propagation of the uncertainties in the independent variables. The systematic error of the ps-TALIF measurements was mainly determined by the uncertainties in the two-photon absorption cross section ratio (50%)^{31,32} and the natural lifetime of xenon (25%),¹⁰ while the largest contributions to the systematic error of THz absorption spectroscopy came from the uncertainties in the line strength (estimated to be maximally 20%) and its temperature-dependence (10%).³⁷ Absolute ground-state atomic oxygen densities including systematic errors are in good agreement for all investigated plasma conditions. For example, for a gas pressure of 1.3 mbar and an applied RF power of 30 W, atomic oxygen densities measured with THz absorption spectroscopy and TALIF were $(7.0 \pm 1.7) \times 10^{14}$ and $(5.3 \pm 3.2) \times 10^{14} \text{ cm}^{-3}$, respectively. The overlap between the results is irrefutable and confirms the validity of both diagnostics.

In this Letter, we have presented a benchmark of THz absorption spectroscopy against a more established method. It has been shown that absolute ground-state atomic oxygen densities measured with THz absorption spectroscopy are in good agreement with those obtained from ps-TALIF measurements. These results demonstrate that THz absorption spectroscopy is a technique with high accuracy that can be reliably used in real-world applications to determine atomic oxygen densities in plasmas.

This work was partially funded by the Leibniz Gemeinschaft (Grant No. K54/2017), the French National Research Agency (ULTRAMAP Project No. ANR-20-CE51-0020), the Île-de-France region (project SESAME DIAGPLAS), and the Department of Science and Technology at the French Embassy in Berlin (Procope Mobility program). In addition, we are grateful to K. Biermann, B. Röben, W. Anders, C. Herrmann, A. Riedel, and A. Tahraoui (all PDI) for fabricating the used THz QCL. Furthermore, we would like to thank H. T. Grahn (PDI) for fruitful discussions and F. Weichbrodt (INP) for technical support.

AUTHOR DECLARATIONS

Conflict of Interest

The authors have no conflicts to disclose.

Author Contributions

Jente Rosemarijn Wubs: Formal analysis (equal); Investigation (equal); Writing – original draft (equal); Writing – review & editing (equal). **Laurent Invernizzi:** Formal analysis (supporting); Investigation (equal); Writing – review & editing (equal). **Kristaq Gazeli:** Formal analysis (supporting); Investigation (equal); Writing – review & editing (equal). **Uwe Macherius:** Formal analysis (supporting); Investigation (equal); Writing – review & editing (equal). **Xiang Lue:** Resources (equal); Writing – review & editing (equal). **Lutz Schrottke:** Resources (equal); Writing – review & editing (equal). **Guillaume Lombardi:** Supervision (equal); Writing – review & editing (equal). **Klaus-Dieter Weltmann:** Supervision (equal); Writing – review & editing (equal). **Jean-Pierre Hubertus van Helden:** Supervision (equal); Writing – review & editing (equal).

DATA AVAILABILITY

The data that support the findings of this study are openly available in INPTDAT at <https://doi.org/10.34711/inptdat.729>, Ref. 38.

REFERENCES

- ¹K.-D. Weltmann and T. von Woedtke, *Plasma Phys. Controlled Fusion* **59**, 014031 (2017).
- ²K. Fricke, H. Steffen, T. von Woedtke, K. Schroeder, and K.-D. Weltmann, *Plasma Processes Polym.* **8**, 51 (2011).
- ³D. Shaw, A. West, J. Bredin, and E. Wagenaars, *Plasma Sources Sci. Technol.* **25**, 065018 (2016).
- ⁴A. Vesel, G. Primc, R. Zaplotnik, and M. Mozetič, *Plasma Phys. Controlled Fusion* **62**, 024008 (2020).
- ⁵A. West, M. van der Schans, C. Xu, M. Cooke, and E. Wagenaars, *Plasma Sources Sci. Technol.* **25**, 02LT01 (2016).
- ⁶X. Yang, Y. C. Kimmel, J. Fu, B. E. Koel, and J. G. Chen, *ACS Catal.* **2**, 765 (2012).
- ⁷E. C. Neyts and A. Bogaerts, *J. Phys. D* **47**, 224010 (2014).
- ⁸K. Bazaka, O. Baranov, U. Cvelbar, B. Podgornik, Y. Wang, S. Huang, L. Xu, J. W. M. Lim, I. Levchenko, and S. Xu, *Nanoscale* **10**, 17494 (2018).
- ⁹U. Cvelbar and M. Mozetič, *J. Phys. D* **40**, 2300 (2007).
- ¹⁰G. D. Stancu, *Plasma Sources Sci. Technol.* **29**, 054001 (2020).
- ¹¹K. Gazeli, G. Lombardi, X. Aubert, C. Y. Duluard, S. Prasanna, and K. Hassouni, *Plasma* **4**, 145 (2021).
- ¹²H. F. Döbele, T. Mosbach, K. Niemi, and V. S. von der Gathen, *Plasma Sources Sci. Technol.* **14**, S31 (2005).
- ¹³D. Steuer, H. van Impel, A. R. Gibson, V. Schulz-von der Gathen, M. Böke, and J. Golda, *Plasma Sources Sci. Technol.* **31**, 10LT01 (2022).

- ¹⁴A. Greb, K. Niemi, D. O'Connell, and T. Gans, *Appl. Phys. Lett.* **105**, 234105 (2014).
- ¹⁵A. Goehlich, T. Kawetzki, and H. F. Döbele, *J. Chem. Phys.* **108**, 9362 (1998).
- ¹⁶K. Niemi, V. S. von der Gathen, and H. F. Döbele, *J. Phys. D* **34**, 2330 (2001).
- ¹⁷X. Lü, B. Röben, K. Biermann, J. R. Wubs, U. Macherius, K.-D. Weltmann, J. H. van Helden, L. Schrottke, and H. T. Grahn, *Semicond. Sci. Technol.* **38**, 035003 (2023).
- ¹⁸L. Schrottke, X. Lü, B. Röben, K. Biermann, T. Hagelschuer, M. Wienold, H.-W. Hübers, M. Hannemann, J. H. van Helden, J. Röpcke, and H. T. Grahn, *IEEE Trans. Terahertz Sci. Technol.* **10**, 133 (2020).
- ¹⁹M. S. Vitiello, G. Scalari, B. S. Williams, and P. De Natale, *Opt. Express* **23**, 5167 (2015).
- ²⁰A. Leitenstorfer, A. S. Moskalenko, T. Kampfrath *et al.*, *J. Phys. D* **56**, 223001 (2023).
- ²¹E. Bründermann, M. Havenith, G. Scalari, M. Giovannini, J. Faist, J. Kunsch, L. Mechold, and M. Abraham, *Opt. Express* **14**, 1829 (2006).
- ²²J. R. Wubs, U. Macherius, K.-D. Weltmann, X. Lü, B. Röben, K. Biermann, L. Schrottke, H. T. Grahn, and J. H. van Helden, *Plasma Sources Sci. Technol.* **32**, 025006 (2023).
- ²³R. Peverall, S. D. A. Rogers, and G. A. D. Ritchie, *Plasma Sources Sci. Technol.* **29**, 045004 (2020).
- ²⁴K. Niemi, D. O'Connell, N. de Oliveira, D. Joyeux, L. Nahon, J. P. Booth, and T. Gans, *Appl. Phys. Lett.* **103**, 034102 (2013).
- ²⁵L. R. Zink, K. M. Evenson, F. Matsushima, T. Nelis, and R. L. Robinson, *Astrophys. J.* **371**, L85 (1991).
- ²⁶K. Gazeli, X. Aubert, S. Prasanna, C. Y. Duluard, G. Lombardi, and K. Hassouni, *Phys. Plasmas* **28**, 043301 (2021).
- ²⁷L. Invernizzi, C. Y. Duluard, H. Höft, K. Hassouni, G. Lombardi, K. Gazeli, and S. Prasanna, *Meas. Sci. Technol.* **34**, 095203 (2023).
- ²⁸K. Niemi, V. Schulz-von der Gathen, and H. F. Döbele, *Plasma Sources Sci. Technol.* **14**, 375 (2005).
- ²⁹S. Schröter, J. Bredin, A. R. Gibson, A. West, J. P. Dedrick, E. Wagenaars, K. Niemi, T. Gans, and D. O'Connell, *Plasma Sources Sci. Technol.* **29**, 105001 (2020).
- ³⁰S.-J. Klose, J. Ellis, F. Riedel, S. Schröter, K. Niemi, I. L. Semenov, K.-D. Weltmann, T. Gans, D. O'Connell, and J. H. van Helden, *Plasma Sources Sci. Technol.* **29**, 125018 (2020).
- ³¹D. J. Bamford, L. E. Jusinski, and W. K. Bischel, *Phys. Rev. A* **34**, 185 (1986).
- ³²C. Drag, F. Marmuse, and C. Blondel, *Plasma Sources Sci. Technol.* **30**, 075026 (2021).
- ³³E. Bisceglia, S. Prasanna, K. Gazeli, X. Aubert, C. Y. Duluard, G. Lombardi, and K. Hassouni, *Plasma Sources Sci. Technol.* **30**, 095001 (2021).
- ³⁴S. Reuter, J. S. Sousa, G. D. Stancu, and J. H. van Helden, *Plasma Sources Sci. Technol.* **24**, 054001 (2015).
- ³⁵I. E. Gordon, L. S. Rothman, R. J. Hargreaves *et al.*, *J. Quant. Spectrosc. Radiat. Transfer* **277**, 107949 (2022).
- ³⁶H. M. Pickett, R. L. Poynter, E. A. Cohen, M. L. Delitsky, J. C. Pearson, and H. S. P. Müller, *J. Quant. Spectrosc. Radiat. Transfer* **60**, 883 (1998).
- ³⁷M. Šimečková, D. Jacquemart, L. Rothman, R. Gamache, and A. Goldman, *J. Quant. Spectrosc. Radiat. Transfer* **98**, 130 (2006).
- ³⁸See <https://doi.org/10.34711/inptdat.729> for "INPTDAT."